

## End-grain bonding of spruce timber at low curing temperatures – effects on tensile strength and how to improve

Dio Lins & Steffen Franke

To cite this article: Dio Lins & Steffen Franke (24 Sep 2024): End-grain bonding of spruce timber at low curing temperatures – effects on tensile strength and how to improve, Wood Material Science & Engineering, DOI: [10.1080/17480272.2024.2403678](https://doi.org/10.1080/17480272.2024.2403678)

To link to this article: <https://doi.org/10.1080/17480272.2024.2403678>



© 2024 The Author(s). Published by Informa UK Limited, trading as Taylor & Francis Group



Published online: 24 Sep 2024.



Submit your article to this journal [↗](#)





View related articles [↗](#)



View Crossmark data [↗](#)

CrossMark

# End-grain bonding of spruce timber at low curing temperatures – effects on tensile strength and how to improve

Dio Lins  and Steffen Franke 

Architecture, Wood and Civil Engineering, Bern University of Applied Sciences, Biel/Bienne, Switzerland

## ABSTRACT

The end-grain bonding of timber components using Timber Structures 3.0 technology (TS3) represents an emerging construction method in the field of timber engineering. For onsite applications, research is being conducted to determine how low temperatures during the curing process affect the bonding and to explore potential methods of mitigating any adverse impacts. The current research results reveal that low curing temperatures detrimentally influence the mechanical properties of the bond. Conversely, investigations into bonding with heated casting resin as a means to counteract the effects of low curing temperatures demonstrate highly beneficial outcomes. Overall, this study provides design-relevant tensile strength values, which, when coupled with suitable application strategies, enable effective bonding under low ambient temperatures. Future investigations will delve deeper into the failure mechanism (adhesion – cohesion) as it relates to curing temperature variations.

## ARTICLE HISTORY

Received 11 July 2024  
Revised 9 September 2024  
Accepted 9 September 2024

## KEYWORDS

End-grain bonded timber;  
low-temperature curing;  
tensile strength; cross-  
laminated timber

## Introduction

### Timber Structures 3.0 technology

Utilising Timber Structures 3.0 technology (TS3), timber components are end-grain bonded in a statically load-bearing fashion. This methodology notably enables the creation of biaxial load-bearing flat slabs constructed from cross-laminated timber (CLT), irrespective of their geometry or size. To achieve this, CLT elements with pre-treated side surfaces are positioned adjacently, maintaining a 4 mm gap. Subsequently, this gap is filled with a casting resin, facilitating a bonding process without the need for lateral pressure. The casting procedure of the joints, which are usually several metres long, is currently implemented in segments, employing sealing strips as separators between them. Injection is conducted via an injection hole positioned at the midpoint of each segment, with injection occurring from bottom to top to prevent air bubble formation (see approval Z-9.1-917 2024). A two-component polyurethane casting resin is employed, similar to that used for bonding steel rods into load-bearing timber components. The TS3 technology thus enables a simple and bending-resistant onsite connection of CLT elements and thus, for the first time, the efficient use of the biaxial load-bearing capacity of this timber construction product.



### Low curing temperatures

The aforementioned approval Z-9.1-917 (2024) for the TS3 technology also specifies that the air temperature during application must be at least 17 °C until the final strength of the TS3

joint is reached. This requirement is attributed to the adhesive used, which was developed based on the adhesive for bonded-in threaded rods in load-bearing timber components according to Z-9.1-896 (2020). Given that the minimal processing temperature is also set as 17 °C in that context, this specification is initially adopted to ensure a quality-assured bonding. However, this requisite presents a challenge for the implementation of TS3 technology. Unlike bonded – in rods, this technology is applied and cured on construction site, where it is exposed to ambient temperatures. It is known that the required temperature of 17 °C is rarely, if ever, achieved during colder seasons in certain parts of the European construction sector, particularly in regions like Scandinavia with its strong affinity for timber construction, but also in the Baltic States and in Central Europe. Consequently, to establish the TS3 technology internationally and thus create a top-quality, climate-neutral substitute for reinforced concrete slabs, it is imperative to understand the effects of low curing temperatures (i.e. below 17 °C) on end-grain bonding and, subsequently to devise practical solutions that extend the applicability of this technology without being limited to the summer season.

### State of the art

When assessing adhesively bonded joints in timber engineering, up to nine distinct failure zones can be identified according to Marra (1992). However, it necessitates a comprehensive evaluation of at least three different “strengths” and their associated failure modes: cohesive strength, adhesive strength, and wood strength. Cohesive strength signifies the inherent

**CONTACT** Dio Lins  dio.lins@bfh.ch  Architecture, Wood and Civil Engineering, Bern University of Applied Sciences, Solothurnstrasse 102, Biel/Bienne 2504, Switzerland

© 2024 The Author(s). Published by Informa UK Limited, trading as Taylor & Francis Group  
This is an Open Access article distributed under the terms of the Creative Commons Attribution License (<http://creativecommons.org/licenses/by/4.0/>), which permits unrestricted use, distribution, and reproduction in any medium, provided the original work is properly cited. The terms on which this article has been published allow the posting of the Accepted Manuscript in a repository by the author(s) or with their consent.

strength of the adhesive itself and is thus a fundamental component of adhesive bonding. Conversely, adhesive strength is defined as the connection at the interface between the adhesive and the wood surface to which it adheres. There are various adhesion theories, of which mechanical interlocking and adsorption in timber construction are probably the most important (cf. Pizzi 1992; Gardner *et al.* 2015). In addition to the natural wood properties (species, density, moisture content, fibre direction), the adhesive strength fundamentally relies on the condition of the wood surface, encompassing factors such as surface roughness or cleanliness. The properties of the adhesive, such as viscosity, also play a significant role. Adhesive strength (Basin and Berlin, 1970) assumes a pivotal role in guaranteeing the longevity of the bond between timber components (Gardner *et al.* 2015). Wood failure as the third failure mechanism, is inherently governed by the mechanical and wood-specific attributes of the timber elements to be joined (Dinwoodie 1975).

Butt joint bonding on the end-grain, incorporating TS3 technology, undergoes continuous development in various research projects from 2010 onwards. Numerous academic theses, including bachelor's, master's, and doctoral dissertations, have significantly contributed to the present-day system (e.g. Schawwalder 2013; Themessl 2018). Additionally, independent research on butt joint bonding on the end-grain exists beyond the scope of TS3 technology. Follrich *et al.* specifically investigated diverse factors influencing bonding, such as grain angle (2007), density (2008), and surface treatments (2007 and 2009). The utilisation of one-component adhesives, coupled with a pressure of 0.7 MPa, though represents a fundamentally distinct bonding system compared to TS3 technology. Bröker and Korte (1994), on the other hand, explored bonding using two-component epoxy resin adhesives, omitting pressure. The study involved testing butt joints with joint thicknesses ranging from 1 mm to 10 mm, representing a system that is very similar to TS3 technology. However, investigation into curing at low temperatures was not undertaken.

In adhesive technology, the enthalpy-supported curing degree, denoted as  $\alpha$  (Prime 1973; Voß and Vallée 2022), is used to describe the curing process, often referred to as curing kinetics, of adhesives. This curing kinetics display a significant temperature dependency and can rely on a variation of Arrhenius' law (Laidler 1984). Initially, the degree of cure does not provide insights into the development of the adhesive's strength or stiffness. The relationship between the curing degree and these mechanical attributes has seen limited exploration. Moussa *et al.* (2012) are among the researchers who initiated preliminary investigations in this area, focusing on the cohesive properties of two-component epoxies and not delving into the adhesive characteristics of timber bonding.

Extensive initial investigations on the mechanical effects of low curing temperatures on end-grain bonded timber connections were previously conducted by Lins *et al.* (2024). Their research revealed that end-grain bonded timber predominantly exhibits adhesive failure. Consequently, both cohesive and adhesive strength were examined as a function of curing time and temperature. The study confirmed that the curing temperature has a decisive influence on the development of both strengths. Even though the exact strength development

curves differ between the two, it is evident that the strength development at low temperatures takes significantly longer than, for example, at 20 °C. Particularly with regard to the wooden (end-grain bonded, adhesive strength) test specimens, the ultimate strength was observed to be lower at reduced curing temperatures. It's crucial to note that the tensile tests were conducted on diminutive test specimens free of wood defects, including knots. Additionally, these tests were executed with relatively modest sample sizes. Therefore, while they provide insight into qualitative performance, they are not suitable for determining characteristic final strengths for design purposes. Furthermore, investigations were carried out by Lins and Franke (2022) to compensate for low curing temperatures during the end-grain bonding of timber components with the aid of milled heating wires. Numerical simulations and experimental validations were used to determine the temperature profile in the casting resin joint in order to be able to adjust the heating wire sensibly according to the boundary conditions at the construction site (temperature, geometry, etc.) so that the required curing temperature can be guaranteed despite low ambient temperatures.

Beyond that, while no publications specifically address the consequences of low curing temperatures on end-grain bonding of timber components, there is existing research on low temperature curing of bonded-in threaded rods. For instance, studies by Kohl *et al.* (2017), Ratsch *et al.* (2022), and Voß *et al.* (2023) have explored methods such as resistive heating and inductive heating. However, it is worth noting that the latter publications do not delve into the implications of low temperatures on the bonding strength, particularly in the context of end-grain bonding. Instead, they primarily focus on methods to achieve the required temperatures temporarily and in a localised manner. It is also essential to recognise that these measures may have limited practical feasibility for on-site applications of end-grain bonding in construction.

### Scope of this article

This study seeks to determine the curing characteristics of the end-grain bonding of timber components, specifically focusing on the impact of low curing temperatures on the tensile strength. Furthermore, it is examined whether casting with heated casting resin, as a compensatory measure for low curing temperatures, yields positive effects. The investigated variants are being carried out extensively to provide statistically robust design-relevant characteristic tensile strength values. In conjunction with other temperature-related design specifications identified in this article, the objective is to facilitate the integration of TS3 technology, including low-temperature design, into quality-assuring design standards, such as EN 14080 (2013) for universal finger joints, as soon as possible.

## Material and methods

### Experimental programme

The experimental programme envisioned curing test specimens at various (low) temperatures (20 °C; 5 °C; 0 °C; see Table 1) to determine the curing characteristics of end-grain

**Table 1.** Overview climatic conditions per series.

| Series Name | Curing Temperature (°C) | Wood Temperature (°C) | Casting Resin Temperature at Injection (°C) | Relative Humidity (%) |
|-------------|-------------------------|-----------------------|---|-----------------------|
| 20 °C wGH   | 20                      | 20                    | 35  | 65                    |
| 20 °C       | 20                      | 20                    | 20  | 65                    |
| 5 °C wGH    | 5                       | 5                     | 35  | 64                    |
| 0 °C wGH    | 0                       | 0                     | 35  | 64                    |
| 0 °C        | 0                       | 0                     | 20  | 64                    |

bonded timber components under such conditions. It was ensured that the wood itself was also already at the appropriate low temperature when it was poured, in order to reflect construction site practice as closely as possible. Furthermore, casting resin with different temperatures (20 and 35 °C; see Table 1) was used for the bonding. The 20 °C warm casting resin represents the “normal case”, whereas the 35 °C warm casting resin (= wGH) was tested as a compensation measure for low curing temperatures. Subsequently, at least 16 tensile tests were carried out for each series on the (1st) / 2nd / 3rd / 4th / 7th / 10th and 15th day after casting (see Table 2) to determine the corresponding tensile strength.

To offer a comprehensive overview of the experiments previously discussed, the following tables provide a detailed breakdown of the climatic and other boundary conditions of the experimental programme.

**Table 2.** Boundary conditions of all series.

|                          |  |
|--------------------------|--|
| Strength Class           | T14 / C24  |
| Density                  | 420 kg/m <sup>3</sup> ± 25 kg/m <sup>3</sup>   |
| Target Moisture Content  | 12 M %   |
| Tested Cross-Section     | 38 mm x 120 mm   |
| Length                   | 800 mm   |
| Adhesive Layer Thickness | 4 mm   |
| Quantity                 | 16 test specimens per test day and series  |
| Test Setup               | Uniaxial tensile tests according to EN 408 + A1 (2012) in conjunction with EN 14080, Annex E2 (2013) |
| Test Speed               | 0.015 mm/s   |
| Test Days                | (1); 2; 3; 4; 7; 10; 15  |

## Materials

In the study, all timber specimens were constructed using spruce timber (*Picea abies*) belonging to the strength class T14 / C24 in compliance with EN 338 (2016). In order to isolate the impact of temperature, every other potential factor affecting tensile strength was minimised to the greatest extent possible. This encompassed maintaining a well-defined density of 420 kg/m<sup>3</sup> with minimal variation, not exceeding ± 25 kg/m<sup>3</sup>. Additionally, a wood moisture content of 12% was the target for all test series. This was accomplished by adjusting relative humidity in accordance with the respective temperature conditions to achieve a wood moisture equilibrium of 12%, as per the methodology established by Keylwerth and Noack (1964). Although the presence of wood defects, especially knots in the casting surface, has a significant influence on the tensile strength of end-grain bonded test specimens, knots were not initially excluded in order to be

able to generate design-relevant absolute tensile strength values. However, for subsequent evaluation of the knot influence, the knot percentages were systematically recorded after the tensile tests.

The adhesive employed was a two-component polyurethane, specifically the proprietary casting resin “TS3 PTS CR192” developed by TS3 for the purpose of bonding timber components at the end-grain. This adhesive is produced without the incorporation of solvents or formaldehyde.

## Test specimen and production

In the preparation of the end-grain bonded timber joints, initially, glued laminated timber (GLT) elements were fashioned from 18 board lamellae (43 mm x 132 mm) each, with a length of 800 mm (cf. Figure 1). This process yielded structural glulam blocks characterised by a uniform alignment of annual rings. Subsequently, these elements were cut once more in the middle of their length. The bonding surfaces were pre-treated with a more viscous variant of the adhesive utilised for the bonding process. After the pre-treatment was allowed to dry for one day at 20 °C and 65% r. h., the halved blocks were exposed to the subsequent (cold) climate in a climate chamber for the next two days until casting. Afterwards, they were conjoined at room temperature with a 4 mm adhesive layer. In this process, care was taken to ensure that always different origin glulam elements were bonded together. The casting process was performed on lying GLT blocks and entailed injection through an injection hole positioned at the centre of the outer lamella (relative to its width). Starting from the injection hole, the individual lamellae were numbered chronologically so that their position in relation to the injection hole could be traced later (see Figure 1 and Figure 2). Immediately after casting, during which the test specimens were exposed to room temperature for about 30 minutes, they were again exposed to the appropriate climate in the climate chamber until they were tested.

For the tensile tests, one end-grain bonded glulam block per test day was removed from the climate chamber and cut apart along the GLT glue joints. The resulting test specimens were then also trimmed on the narrow sides (approx. 6 mm per side, see Figure 1). The outer lamellae of the block (= cover lamellae) were not tested, resulting in 16 test specimens each with a cross-section of 38 mm x 120 mm (see Figure 3).

The complexity of the test specimen production process arose from the need to eliminate potential edge-related influences, including the formation of surface bubbles or incomplete casting. Although these factors are usually of little consequence in larger components, they can lead to a significant influence on tensile strength in smaller specimens.

## Uniaxial tensile tests

The tests were performed in a horizontal tensile testing machine. This is assigned to class 1 of the machine range according to EN ISO 7500-1 (2018) (including a maximum relative error of ± 1% of the force-measuring system).

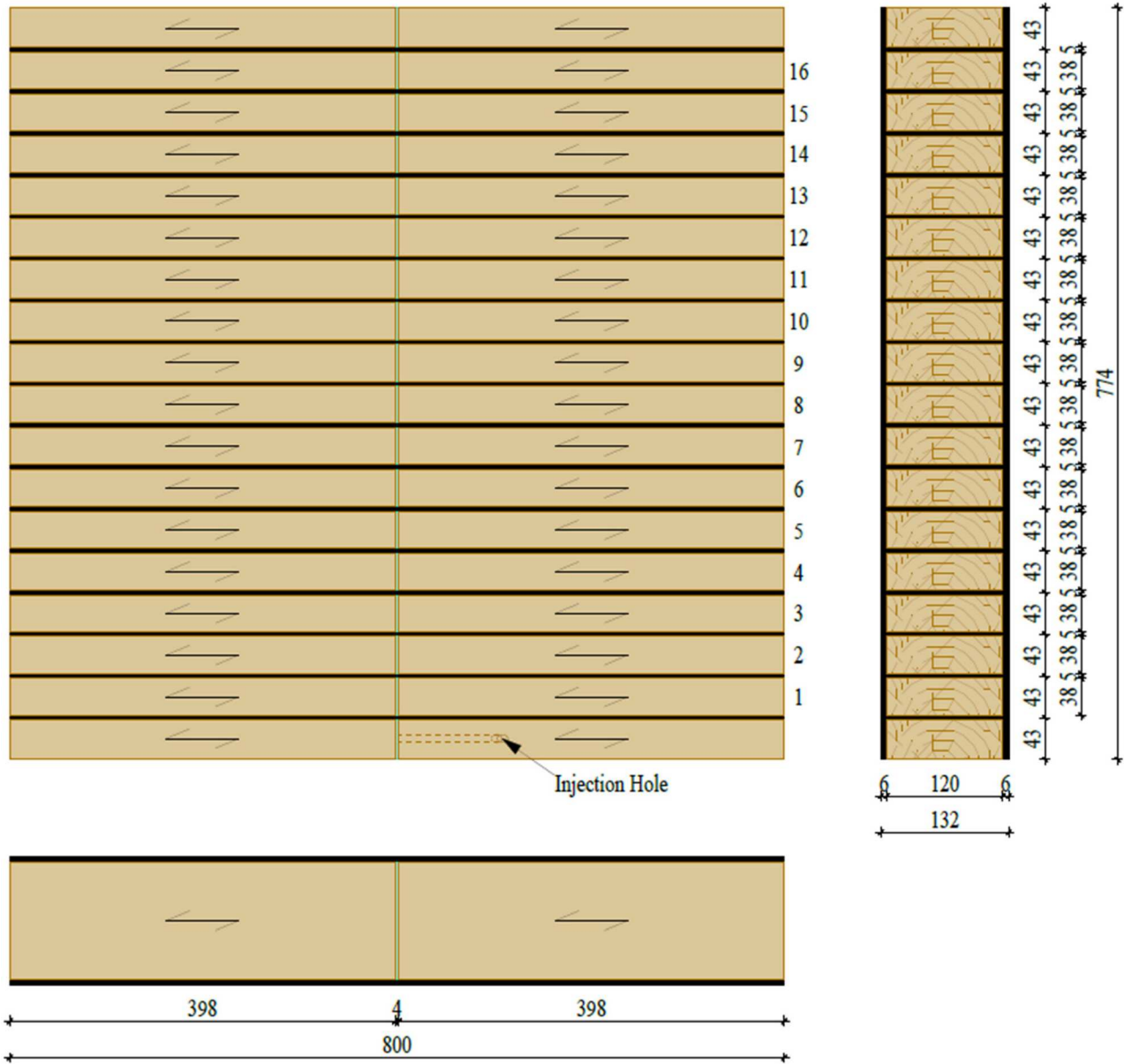


**Figure 1.** Views & top view of the end-grain bonded glulam element incl. cutting plan (black lines = cutting lines); all dimensions in (mm).



**Figure 2.** End-grain bonded glulam element: circle = injection hole; upper rectangle = casting resin joint; lower rectangle = numbering of the lamellae.

The test setup of the uniaxial tensile tests was based on EN 408 + A1 (2012) in conjunction with EN 14080, Annex E2 (2013). The test specimens had a free length of about 200 mm per side

(= 400 mm  $\geq$  9 x width, see Figures 4 and 5). During the execution, the temperature was between 17 and 29 °C and the relative humidity between 35% and 65%. The tests were conducted displacement-controlled with a test speed of 0.015 mm/s.

The tensile strengths  $f_{t,0}$  were calculated according to EN 408 + A1 (2012) using the following equation (1):

$$f_{t,0} = \frac{F_{max}}{A_{joint}} \quad (1)$$

## Results

### Impact of the distance to injection hole and curing time

Firstly, it is noteworthy that the examined specimens predominantly failed at the adhesive-timber interface (adhesive failure mode, see Figure 6). To assess the effects of curing time and the tested lamella's distance from the injection hole, herein-after simplified referred to as distance, on the tensile strength,

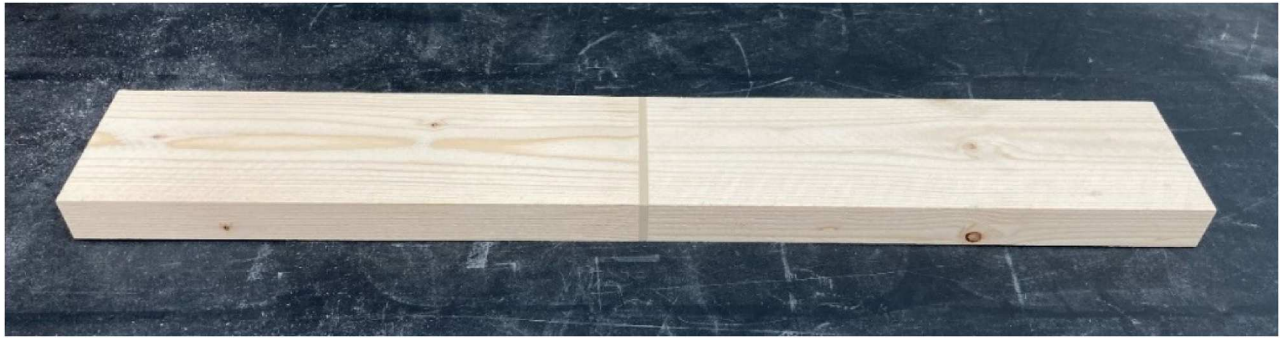


Figure 3. Pre-cut test specimen.

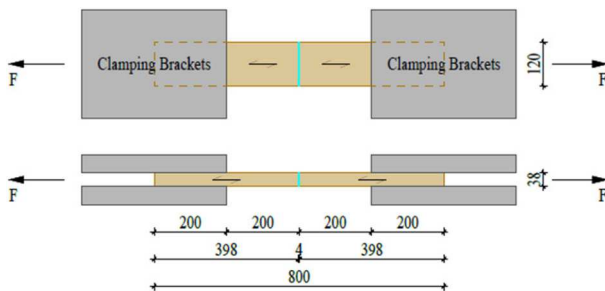


Figure 4. Schematic structure tensile test; all dimensions in (mm).



Figure 5. Test specimen in the tensile testing machine.



Figure 6. Representative adhesive failure mode.

only those test specimens that show no knots on the fracture surface are initially being analysed. When coupled with the homogenisation methods outlined in *Material and methods*, these influences can be considered as isolated to the greatest extent possible.

The three-dimensional plots in Figure 7 depict the tensile strength in relation to both the distance and curing time. The individual values have been connected by a smoothed and coloured surface to make the dependencies easier to see. At a curing temperature of 20 °C, whether employing warm (35 °C) or normal (20 °C) casting resin, no substantial impact of curing time or distance is observed (see Figure 7 a) and b)). However, at lower curing temperatures, there is a visible influence of both curing time and distance. The tensile strength exhibits an increase with prolonged curing time and a decrease with greater distance. Notably, no perceptible systematic variation within the individual series is evident in the impact of distance on tensile strength concerning time, or conversely, in the influence of time in relation to distance (see Figure 7 c), d) and

e)). In simple terms, there is no systematic relationship between curing time and distance.

Hence, in the context of the tensile strength plotted against the time-averaged distance (including standard deviation), as depicted in Figure 8, no significant data is lost, but it is possible to analyse the influence of distance in much finer detail. This further emphasises that, at a curing temperature of 20 °C, the distance to the injection hole shows no influence on tensile strength, as indicated by the continuous line representing the overall average value of each series (refer to Figure 8 a)). Nonetheless, at lower curing temperatures, this influence becomes distinctly obvious and can be suitably represented by third-degree polynomial functions for each of the three test series. The selection of this type of function is based on two key criteria. Firstly, it correlates to a high degree with the empirical data (e.g.  $R^2$  for the 0 °C series = 0.95), and secondly, it forms a basis for the subsequent measures by defining inflection points. Overall, it is apparent that both a lower curing temperature and a reduced casting resin temperature increase the negative impact of the distance (see Figure 8 b)).

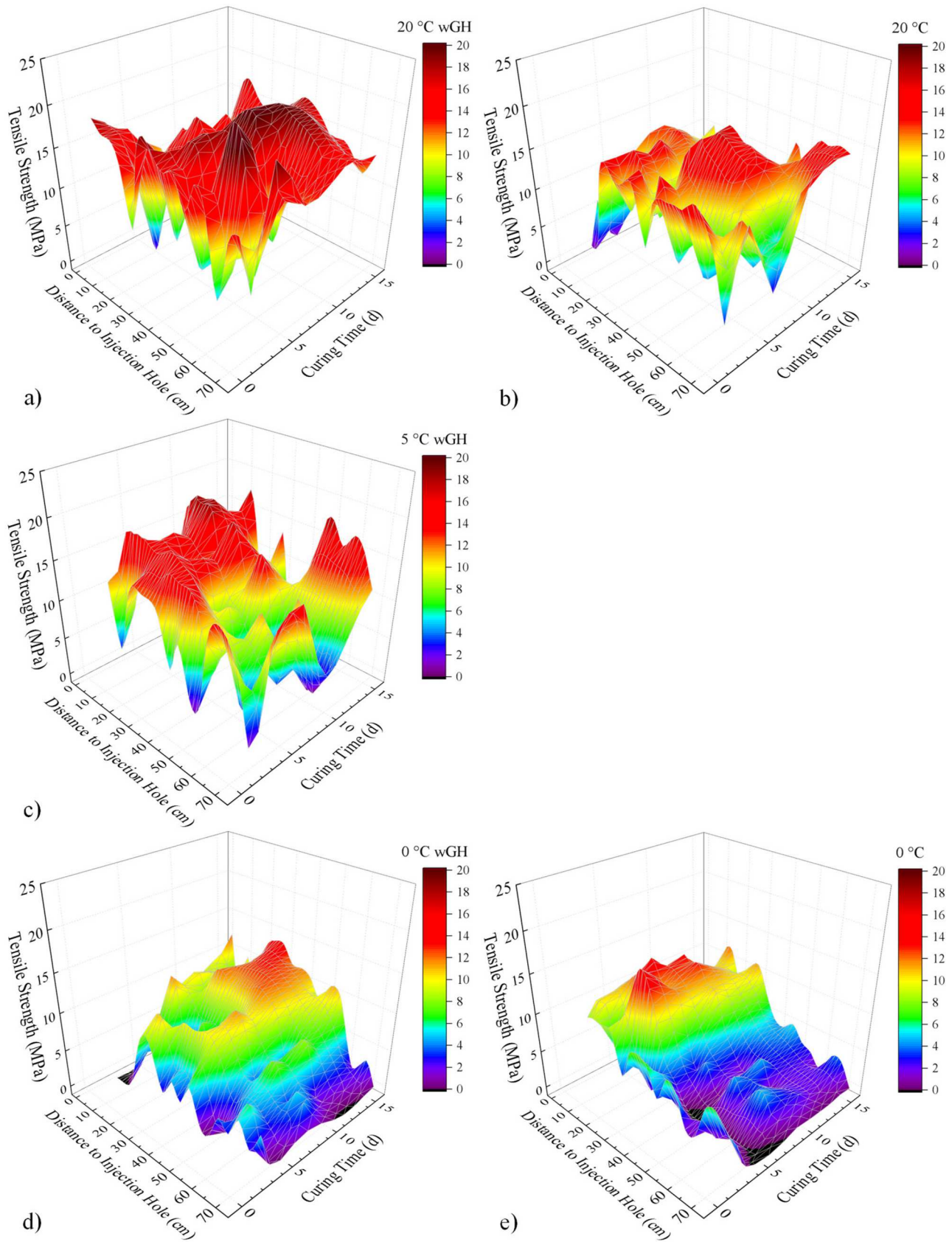


**Figure 7.** Tensile Strength vs. Distance to Injection Hole vs. Curing Time incl. smoothing: 20 °C wGH series (a); 20 °C series (b); 5 °C wGH series (c); 0 °C wGH series (d); 0 °C series (e).

As a straightforward means to restrict the adverse influence of the distance, it is evident that reducing the segment lengths presents a rational approach. Consequently, a specification for

the maximum segment length in relation to the curing and casting resin temperature is now established. As previously indicated, the inflection points of the polynomial functions

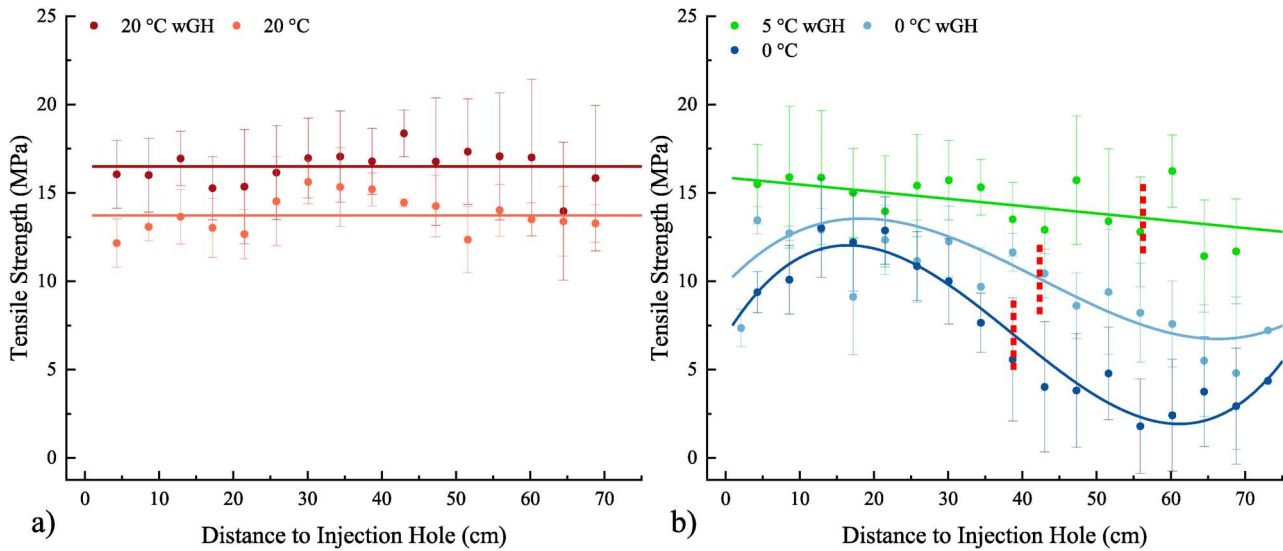


**Figure 8.** Tensile Strength vs. Distance to Injection Hole incl. standard deviation and trendlines: 20 °C wGH & 20 °C series (a); 5 °C wGH, 0 °C wGH & 0 °C series (b); red markings = inflection points.

are selected for this purpose, as illustrated by the red markings in Figure 8 b). Thus, Figure 9 only takes those test specimens originating from the area between the injection hole and the respective inflection point of the polynomial function (5 °C wGH  $\approx$  55 cm; 0 °C wGH  $\approx$  45 cm; 0 °C  $\approx$  40 cm) into consideration. It graphically illustrates the mean values of tensile strength obtained this way, complete with standard deviation, in relation to curing time. Additionally, the data points are modelled utilising an exponential function to replicate the observed patterns. This function posits that each dataset, corresponding to a specific test series, converges towards a final value ( $\sigma_{\infty}$ ) in accordance with an exponential growth function as defined by equation (2). In this context, the term ‘ $t_1$ ’ signifies a characteristic time constant at which about 63% of the final strength is attained. Observations reveal that curing at a temperature of 20 °C, regardless of the casting resin temperature, progresses rapidly, with the attainment of final strength occurring in approximately one day. Moreover, it can be affirmed that, under identical casting resin temperature conditions, curing decelerates as curing temperature decreases, concurrently leading to a lower final strength. Additionally, the curing rate exhibits a slight reduction at the same curing temperature when casting resin temperature is increased, but this leads to a higher final strength.

$$\sigma(t) = \sigma_{\infty}[1 - e^{-t/t_1}] \quad (2)$$

### Empirical final strengths

For the assessment of the final strengths, only the lamellae situated within the previously defined limit distances (cf. Figure 8) are considered. Beyond that, the time at which  $\approx$  99% of  $\sigma_{\infty}$  is reached is calculated for each test series according to equation (2). Following this, only lamellae that underwent testing from this point onwards (20 °C wGH & 20 °C = day 1; 5 °C wGH & 0 °C = day 7; 0 °C wGH = day 10) are employed in the evaluation. Conversely, the corresponding test specimens exhibiting knots in the fracture surface, which were previously excluded,

are now incorporated. Since no other test specimens, such as outliers, are excluded, relevant tensile strength values for design purposes can be provided. The values determined through this method are displayed in Figure 10, categorised by test series, depicted as traditional boxplots including all individual data points. Additionally, mean values are presented as numerical figures alongside the boxes. The boxplots provide clear evidence, consistent with the findings in Figure 9, that decreased curing temperatures at the same casting resin temperature result in significantly lower mean final strength values (significance proven using individual t-tests or Welch’s t-tests to account for heteroscedasticity). Roughly 20% strength reduction is observed between 20 and 0 °C curing temperature, regardless of the casting resin temperature. Similarly, under identical curing temperature conditions, higher average final strengths are achieved with a greater casting resin temperature. This increase amounts to approximately 20% at both 0 and 20 °C curing temperature and it is also statistically significant. In addition to the findings related to strength, it is worth noting that the scatter of the individual test series exhibits some differences. However, no discernible systematic correlation between curing or casting resin temperature and this variability is evident. Notably, the 0 °C wGH series stands out, displaying a relatively low coefficient of variation (COV) at 13%, as indicated in Table 3.

### Characteristic strengths according to EN 14358 (2016)

#### Determination of distribution and characteristic values

When calculating the characteristic tensile strength values (5% quantiles) in accordance with EN 14358 (2016), the initial step involves determining the distribution functions. For this purpose, the empirical final tensile strengths, as elaborated before, are tested individually for each test series, considering both the normal and the lognormal distribution, since the standard distinguishes between these two distributions. An effective tool for determining the distribution function is the



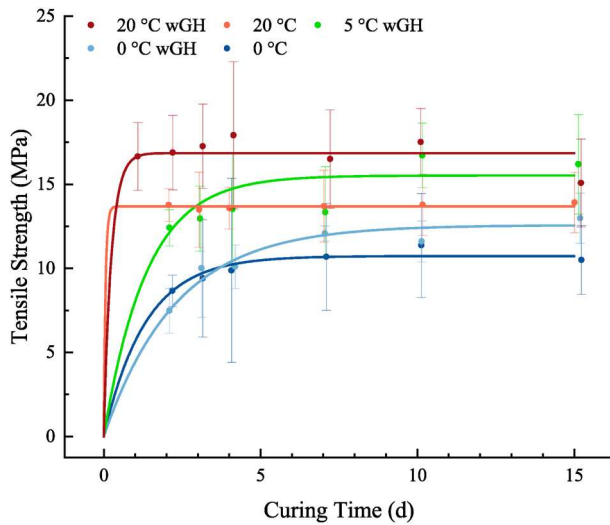


**Figure 9.** Tensile Strength vs. Curing Time incl. standard deviation and trendlines for all series.

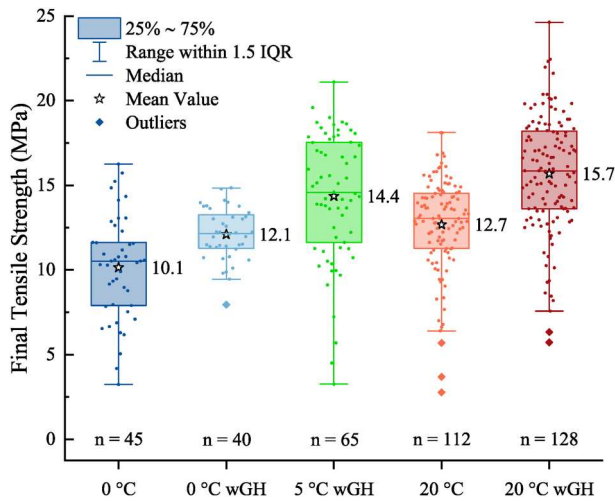


**Figure 10.** Boxplots of the Final Tensile Strengths for all series.

**Table 3.** Determined values according to EN 14358 (2016) for normal distribution.

| Series Name | Mean Value (MPa) | Standard Deviation (MPa) | COV (%) | 5% Quantile (MPa) |
|-------------|------------------|--------------------------|---------|-------------------|
| 20 °C wGH   | 15.69            | 3.43                     | 22      | 9.58              |
| 20 °C       | 12.68            | 2.79                     | 22      | 7.71              |
| 5 °C wGH    | 14.36            | 3.80                     | 26      | 7.51              |
| 0 °C wGH    | 12.09            | 1.54                     | 13      | 9.26              |
| 0 °C        | 10.15            | 3.05                     | 30      | 4.58              |

utilisation of QQ-plots (refer to Figures 11 and 12). These plots involve a comparison between theoretical quantiles and actual quantiles, with the agreement being subsequently evaluated. Within the diagrams, the black line denotes the ideal normal or lognormal distribution, while the light blue area represents the 95% confidence interval (CI) for the respective distribution. The examination for normal distribution (Figure 11) shows that the data points largely conform to a normal distribution. The majority of values are falling within the 95% CI with only a

few exceptions noted within the 20 °C and 5 °C wGH series. Conversely, when assessing the lognormal distribution (Figure 12), there is a systematic deviation from the linear trend, indicating that the data does not conform to this distribution. Notably, a substantial portion of the data points falls outside the confidence interval in this scenario. Consequently, it is assumed that the tensile strength of the TS3 connection conforms to a normal distribution. The Kolmogorov–Smirnov test verifies this at a 5% significance level for all test series. Thus, the characteristic values displayed in Table 3 are calculated in accordance with EN 14358 (2016) for normally distributed data.

### Analysis in relation to curing and casting resin temperature

The characteristic values of the final tensile strength, as previously presented in Table 3, are graphically represented in Figure 13. In this figure, these values are plotted against the curing temperature as asterisks. Distinct colours are used to differentiate between the two casting resin temperatures (35 °C = red; 20 °C = blue). Furthermore, the idealised normal distributions resulting from the empirical mean values and standard deviations are displayed. Alongside the values determined in this study, the characteristic tensile strength value established as part of the approval process is also depicted. This value is represented as a green dashed line in the graph and was determined by MPA University of Stuttgart (see Gutachterliche Stellungnahme (2022)) for board lamellae with similar dimensions. Since the approval process did not include an investigation of low curing temperatures, this value in the design is exclusively applicable for curing temperatures of at least 17 °C. Nevertheless, it serves as a benchmark value for lower curing temperature scenarios in this context.

Consistent with the empirical data, which have been predominantly analysed concerning mean values in *Empirical final strengths*, a fundamental principle can be deduced. Higher casting resin temperatures, under identical curing conditions, result in significantly increased characteristic tensile strengths within the examined range. Additionally, a curing temperature of 0 °C results in approximately a 40% reduction in characteristic strengths when compared to a curing temperature of 20 °C, assuming a casting resin temperature of 20 °C. However, in contrast to the mean value level, this relationship is not consistently observed when the casting resin temperature is set at 35 °C. In this scenario, the characteristic strength at a curing temperature of 0 °C nearly matches that at 20 °C and surpasses the strength at 5 °C curing temperature. This outcome is primarily attributed to the comparatively low statistical dispersion observed in the 0 °C wGH series.

When comparing with the approval data, it is noteworthy that this study's 20 °C series underwent testing under comparable environmental conditions as those utilised during the approval process. Furthermore, also the 5% quantile derived from this study aligns closely with that observed in the approval data, enhancing the overall credibility of the results. In comparison, the 0 °C series displays a significantly lower strength. Conversely, the series with a casting resin temperature of 35 °C either exhibit higher (0 °C wGH and 20 °C wGH series) or nearly identical (5 °C wGH series) strengths compared to the benchmark series.

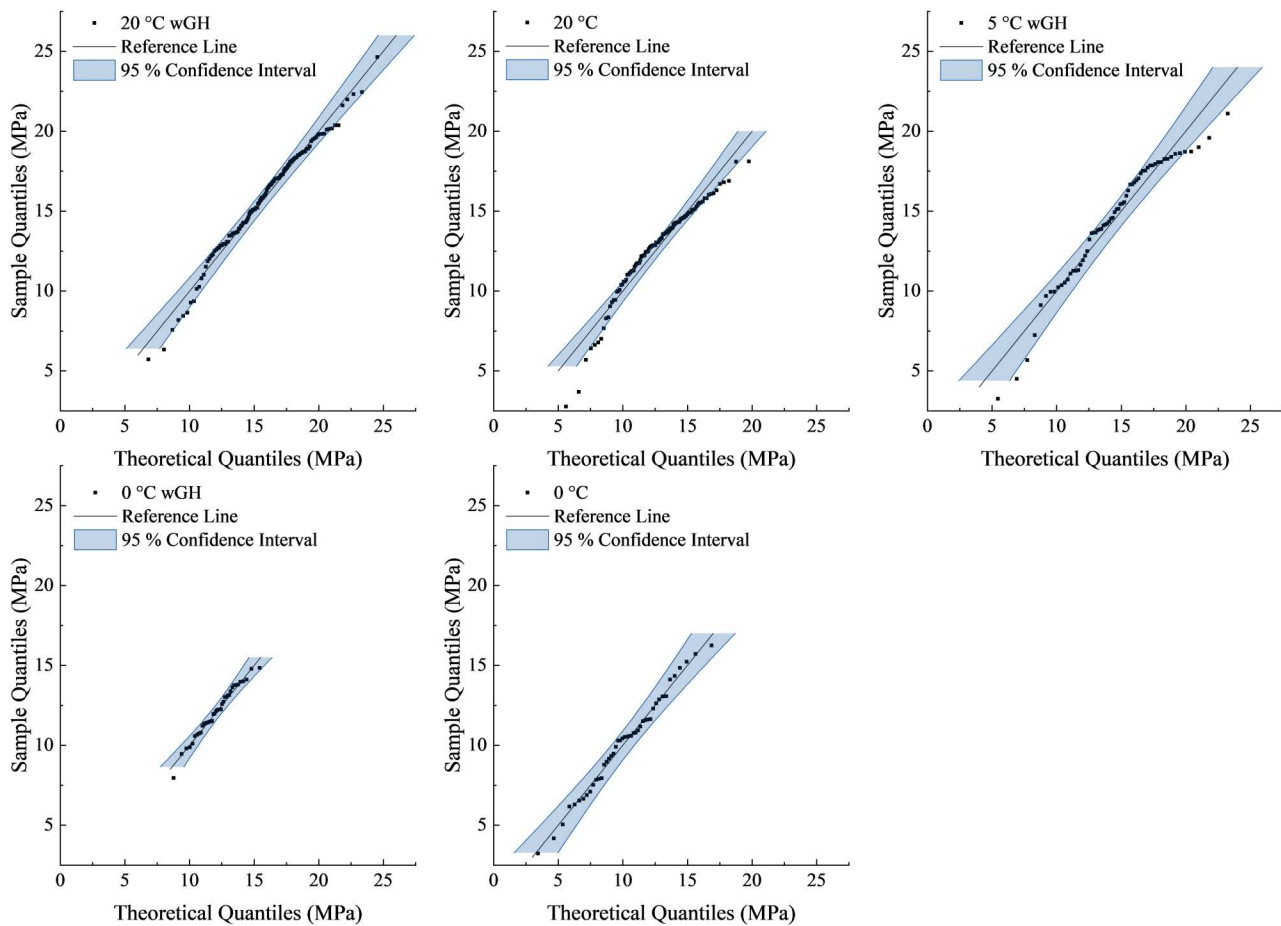


**Figure 11.** QQ-plots: Test for normal distribution for all series.

## Discussion

The observed impact of the distance of the tested lamellae from the injection hole appears highly plausible. The farther a lamella is from the injection hole, the longer the casting resin, which is warmer than the wood, must flow to reach it. It passes the cold wood and continues to cool down. Accordingly, the achieved tensile strength also decreases with increasing distance. In the test specimens examined in this study, the injection hole was located in the outer lamella of a glulam element, whereas in practice, it is typically positioned in the middle of a CLT segment. Therefore, it is assumed that the maximum distances determined here can be applied in both directions from the injection hole when used on construction sites, doubling the potential segment lengths. It is also assumed that the strengths determined are on the conservative side, given that cooling from the lateral edges is less pronounced under real conditions than in the laboratory setting. This is due to the presence of neighbouring segments, which act as a barrier to the cooling process in practice.

Concerning the strength development, it is plausible that lower curing temperatures result in a slower curing process and a reduction of the final strengths. Conversely, a higher casting resin temperature leads to higher final strengths. However, counter-intuitively, the development of strength

seems to be slowed down by a higher casting resin temperature, at least at low curing temperatures.

Also counter-intuitive is the fact that the tensile strength of the TS3 joint follows a normal distribution, whereas the tensile strength of strength-graded timber is usually log-normally distributed. However, this is primarily attributed to the sorting process, wherein strength-reducing wood characteristics such as knots are sorted out based on the targeted strength class. Conversely, the highest strengths are not limited by grading, resulting in a lognormal distribution. Although the lamellae used in this study underwent the same sorting (with additional sorting based on density), this distribution of strength is not mirrored in the TS3 joint. The reason for this discrepancy is that the tensile strength of wood in its pure form is notably higher than that of the TS3 joint as it fails in the adhesive-timber interface. Consequently, its strength distribution essentially relies on the frequency of wood defects in this interface. Nevertheless, the local distribution of wood features in the test specimen is normally distributed and does not impact the pure wood tensile strength distribution due to the constant stress distribution. It is also conceivable that the strength distribution of the TS3 joint results from the raw density distribution of the wood, which is also normally distributed.

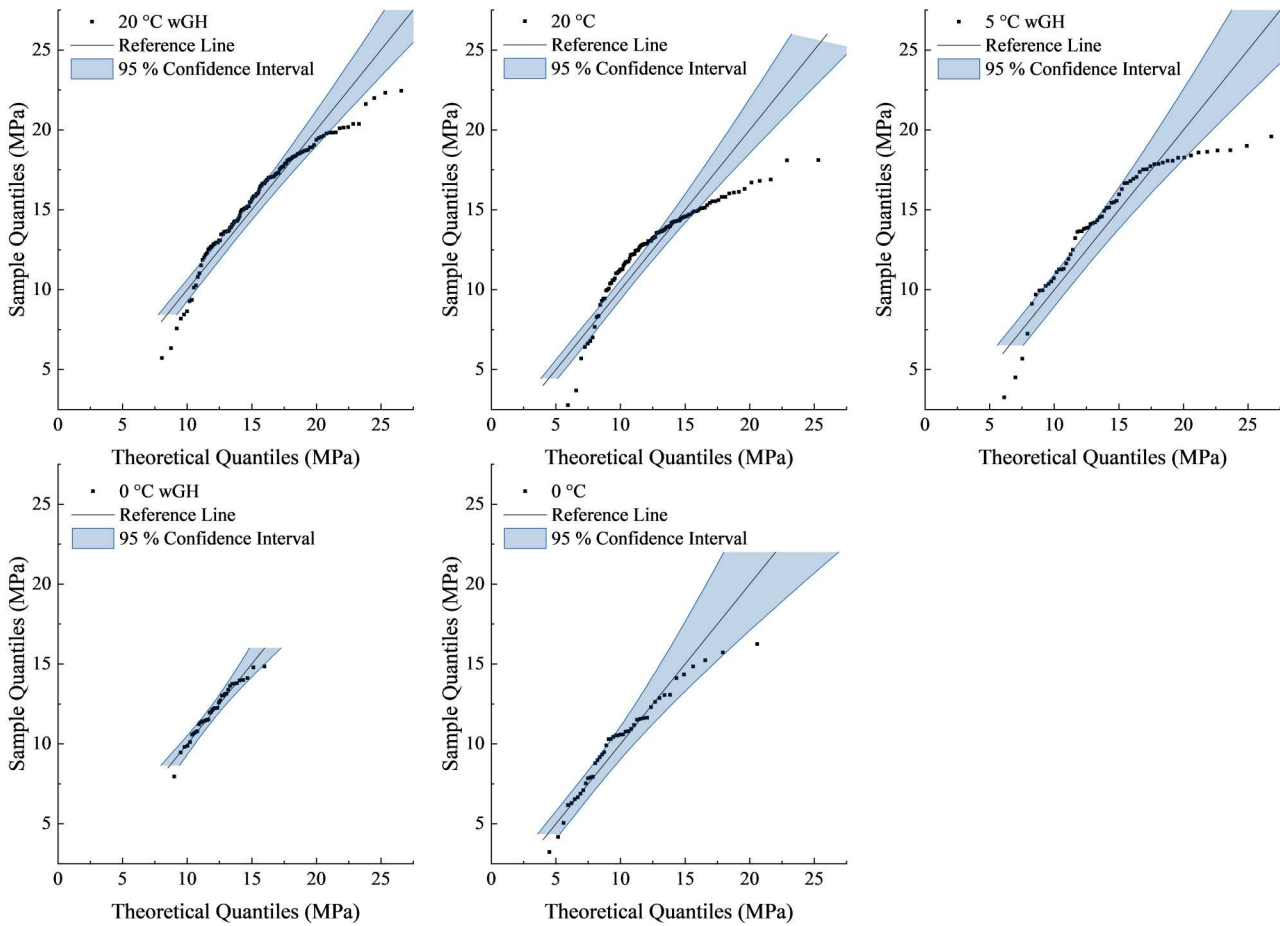


Figure 12. QQ-plots: Test for lognormal distribution for all series.

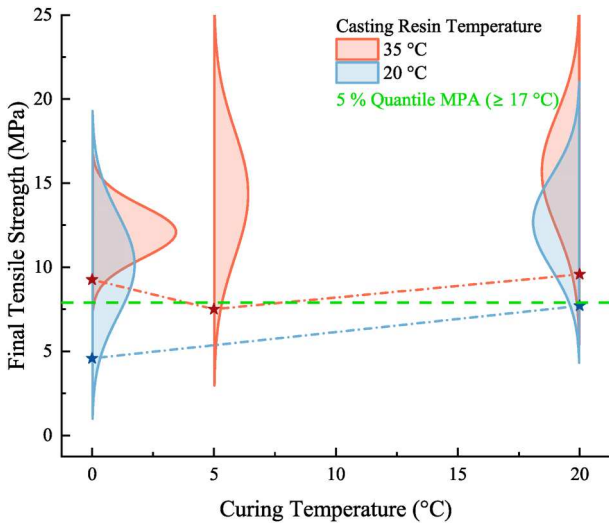


Figure 13. Final Tensile Strength vs. Curing Temperature incl. normal distribution & 5% quantiles according to EN 14358 (2016) for all series.

In comparison to the other series, the 0 °C wGH series exhibits a markedly low standard deviation, whereas the 5 °C wGH series displays a comparatively high deviation. Therefore, contrary to expectations, the corresponding characteristic strengths at a curing temperature of 5 °C are observed to be lower than at 0 °C. The different distributions can be attributed, at least in part, to the slightly varying percentages of

knots in the individual series. The proportion of test specimens exhibiting knots is highest in the 5 °C wGH series and lowest in the 0 °C wGH series. However, the total percentage of knots is less than 2.5% in all series, indicating that the impact is relatively limited. This is also confirmed by the observation that when the final strengths are analysed without knots, the 5% quantiles of the 0 °C wGH and 5 °C wGH series remain approximately at the level of the 20 °C series and the positive influence of a higher casting resin temperature is still statistically significant.

In general, the temperature-dependent viscosity of the casting resin, increasing with decreasing temperature, is considered a possible reason for the final strengths depending on the casting resin and curing temperature, both at empirical and characteristic levels. The hypothesis posits that a higher viscosity results in inferior wetting between the casting resin and the pre-treatment, consequently leading to lower tensile strengths. Conversely, the influence of the pure casting resin’s curing characteristics, as investigated by Lins *et al.* (2024), is not considered to be decisive, as the cohesive tensile strength of the casting resin is higher than that of the TS3 connection for identical curing times and temperatures. This is also reflected in the observation that adhesive failure was the predominant failure mode. Moreover, the relationship between temperature and strength is not presumed to be linear, even if the linear connection of the points in Figure 13 might suggest this.

## Conclusion and outlook

The extensive tests in the study outlined above, focusing on the impact of low curing temperatures on the tensile strength of end-grain bonded timber components, yield far-reaching implications for future on-site bonding using TS3 technology. Firstly, the observations made by Lins *et al.* (2024) are corroborated, indicating that the curing process for TS3 bonding is lengthened at lower temperatures. Furthermore, even with an extended curing period, the tensile strength at low temperatures (while maintaining the same casting resin temperature) generally remains lower than at e.g. 20 °C. Nevertheless, straightforward yet effective measures have been devised to counteract the effects of low curing temperatures.

These measures involve restricting segment lengths (i.e. the chamber sizes cast on-site) and warming up the casting resin to 35 °C before casting. Additionally, the curing times required to achieve the final strengths were determined as a function of the curing and casting resin temperature. The extensive testing enables the provision of robust and reliable characteristic tensile strengths for design purposes. These values validate that casting can be conducted at low ambient temperatures down to 0 °C without a loss of characteristic tensile strength compared to approval tests if the described measures are followed. This is particularly true given that the characteristic tensile strengths specified in the final approval are approximately 25% lower than the benchmark values used to compare this study, providing a good level of safety.

These measures are already being implemented on construction sites in Switzerland, and their efficacy has been validated through quality assurance tests on specimens from the sites. Moreover, the results are intended to be incorporated into an extension of the approval for TS3 technology. In further research activities, the failure mechanism in relation to curing and casting resin temperature will be profoundly analysed. Microscopic analyses will determine the precise interface of fracture occurrence and ascertain whether there are temperature-related differences. Additionally, other variables that may affect the tensile strength of the TS3 joint are being investigated, including the viscosity of the casting resin, to achieve further improvements and increase the load-bearing capacity of the TS3 joint.

## Acknowledgement

The project embodies a collaborative endeavour among Timber Structures 3.0 AG, Schilliger Holz AG, Henkel & Cie. AG, ETH Zürich, and Bern University of Applied Sciences. The authors convey their genuine gratitude for the robust collaboration with the project partners. Furthermore, the authors would like to extend their thanks to Innosuisse for the substantial funding support provided for this ongoing project [Application Number: 50393.1 IP-ENG].

## Disclosure statement

No potential conflict of interest was reported by the author(s).

## Funding

This work was supported by Innosuisse – Schweizerische Agentur für Innovationsförderung.

## ORCID

Dio Lins  <http://orcid.org/0009-0003-2524-9646>

Steffen Franke  <http://orcid.org/0000-0003-2430-8491>

## References

- Basin, V.E., and Berlin, A.A., 1970. Adhesive strength. *Polymer Mechanics*, 266–271. doi:10.1007/BF00859200.
- Bröker, F.W., and Korte, K., 1994. Festigkeiten von Hirnholzverbindungen mit dicken Epoxidharzfugen [Strengths of end-grain connections with thick epoxy resin joints]. *Holz als Roh- und Werkstoff*, 52, 287–292.
- Dinwoodie, J.M., 1975. Timber – a review of the structure-mechanical property relationship. *Journal of Microscopy*, 3–32. doi:10.1111/j.1365-2818.1975.tb04002.x.
- EN 408 + A1, 2012. *Timber structures – structural timber and glued laminated timber – determination of some physical and mechanical properties*. European Committee for Standardization (CEN).
- EN 14080, 2013. *Timber structures – glued laminated timber and glued solid timber – requirements*. European Committee for Standardization (CEN).
- EN 338, 2016. *Structural timber – strength classes*. European Committee for Standardization (CEN).
- EN 14358, 2016. *Timber structures – calculation and verification of characteristic values*. European Committee for Standardization (CEN).
- EN ISO 7500-1, 2018. *Metallic materials – calibration and verification of static uniaxial testing machines – part 1: tension/compression testing machines – calibration and verification of the force-measuring system (ISO 7500-1:2018)*. European Committee for Standardization (CEN).
- Follrich, J., et al., 2007. Tensile strength of softwood butt end joints. Part 1: Effect of grain angle on adhesive bond strength. *Wood Material Science and Engineering*, 83–89. doi:10.1080/17480270701841043.
- Follrich, J., et al., 2007. Tensile strength of softwood butt end joints. Part 2: improvement of bond strength by a hydroxymethylated resorcinol primer. *Wood Material Science and Engineering*, 90–95. doi:10.1080/17480270701850473.
- Follrich, J., et al., 2008. Adhesive bond strength of end grain joints in softwood with varying density. *Holzforschung*, 237–242. doi:10.1515/HF.2008.043.
- Follrich, J., et al., 2009. Comparison of the effect of chemical and mechanical treatment of end-grain surfaces on adhesive bond strength. *Wood Material Science and Engineering*, 98–104. doi:10.1080/17480270903288373.
- Gardner, D.J., et al., 2015. *Adhesion theories in wood adhesive bonding. Progress in Adhesion and Adhesives*, 125–168. doi:10.1002/9781119162346.ch5.
- Gutachterliche Stellungnahme, Berichts-Nr.: 903 4400 000 / 29\_2, 2022. *Allgemeine bauaufsichtliche Zulassung der TS3-Brettsperrholz-Verklebung (TS3-PTS) der Firma Timber Structures 3.0 AG [General building authority approval of the TS3 cross-laminated timber bonding (TS3-PTS) from Timber Structures 3.0 AG]* (confidential). Materialprüfungsanstalt Universität Stuttgart.
- Keylwerth, R., and Noack, D., 1964. *Die Kammertrocknung von Schnittholz [The chamber drying of sawn timber]*. *Holz als Roh- und Werkstoff*, 22, 29–36. doi:10.1007/BF02627726.
- Kohl, D., et al., 2017. Manufacturing gluing-in-rods under low temperatures and with shorter process times using induction and resistive heating. *Welding in the World*, 575–580. doi:10.1007/s40194-017-0432-2.
- Laidler, K.J., 1984. *The development of the Arrhenius equation*. *Journal of Chemical Education*, 494–498. doi:10.1021/ed061p494.
- Lins, D., et al., 2024. Low-temperature adhesive curing in timber engineering: about the relationship between curing kinetics and mechanical properties. *International Journal of Adhesion and Adhesives*, doi:10.1016/j.ijadhadh.2024.103815.
- Lins, D., and Franke, S., 2022. *Simulation of the temperature distribution in glued butt-joint timber connections*. *World Congress on Computational Mechanics*, doi:10.23967/wccm-apcom.2022.104.
- Marra, A.A., 1992. *Technology of wood bonding: principles and practice*. New York: Van Nostrand Reinhold, 454.

- Moussa, O., et al., 2012. Early-age tensile properties of structural epoxy adhesives subjected to low-temperature curing. *International Journal of Adhesion and Adhesives*, 9–16. doi:10.1016/j.ijadhadh.2012.01.023.
- Pizzi, A., 1992. A brief, non-mathematical review of adhesion theories as regards their applicability to wood. *Holzforschung und Holzverwertung*, 44, 6–11.
- Prime, R.B., 1973. Differential scanning calorimetry of the epoxy cure reaction. *Polymer Engineering and Science*, 365–371. doi:10.1002/pen.760130508.
- Ratsch, N., et al., 2022. Accelerated curing of glued-in threaded rods by means of inductive heating – part IV: curing under low temperatures. *The Journal of Adhesion*, 105–130. doi:10.1080/00218464.2020.1818562.
- Schawwalder, A., 2013. *Untersuchungen zu baustellentauglichen Verbindungen mittels Hirnholzverklebungen im Holzbau [Investigations into construction site-suitable connections using end-grain bonding in timber construction]*. Bachelor Thesis. Bern University of Applied Sciences.
- Themessl, A., 2018. *Evaluation zweier Klebstoffsysteme hinsichtlich Zugfestigkeit und Anwendbarkeit bei stumpfer stirnseitiger Verklebung von Fichtenholz [Evaluation of two adhesive systems with regard to tensile strength and applicability for butt end-grain bonding of spruce timber]*. Master Thesis. Bern University of Applied Sciences.
- Voß, M., Evers, T., and Vallée, T., 2023. Low-temperature curing of adhesives – large-scale experiments. *The Journal of Adhesion*, 817–852. doi:10.1080/00218464.2022.2059353.
- Voß, M., and Vallée, T., 2022. Effects of curie particle induced accelerated curing on thermo mechanical performance of 2K structural adhesives – Part I: Bulk properties. *The Journal of Adhesion*, 1298–1339. doi:10.1080/00218464.2021.1909482.
- Z-9.1-896, 2020. *2K-PUR Klebstoff Loctite CR 821 Purbond zum Einkleben von Stahlstäben in tragende Holzbauteile [2C-PUR adhesive Loctite CR 821 Purbond for gluing steel rods into load-bearing timber components]*. Berlin: Deutsches Institut für Bautechnik (DIBt).
- Z-9.1-917, 2024. *Tragend verklebte Brettsperrholzelemente "TS3-PTS-Elemente" für Decken- und Dachkonstruktionen [Load-bearing glued cross-laminated timber elements "TS3-PTS elements" for floor and roof structures]*. Berlin: Deutsches Institut für Bautechnik (DIBt).